Aharonov-Bohm oscillations in the local density of states

A. Cano[1,*] and I. Paul[2,3,†]

[1]*European Synchrotron Radiation Facility, 6 rue Jules Horowitz, BP 220, 38043 Grenoble, France*
[2]*Institut Néel, CNRS/UJF, 25 Avenue des Martyrs, BP 166, 38042 Grenoble, France*
[3]*Institut Laue-Langevin, 6 rue Jules Horowitz, BP 156, 38042 Grenoble, France*

The scattering of electrons with inhomogeneities produces modulations in the local density of states of a metal. We show that electron interference contributions to these modulations are affected by the magnetic field via the Aharonov-Bohm effect. This can be exploited in a simple scanning-tunneling-microscopy setup that serves as an Aharonov-Bohm interferometer at the nanometer scale.

PACS number(s): 73.20.At, 73.23.−b, 73.40.Gk

Scanning tunneling microscopy (STM) provides a powerful tool to measure the density of states.[1] The scattering of electrons with inhomogeneities is known to modify the corresponding density of states producing local modulations. These modulations were first probed by STM with atomic resolution in Ref. 2, where standing-wave patterns in the local density of states (LDOS) arising from scattering of electrons with impurities and step edges were observed on the surface of Cu(111). These patterns encode information about the electronic properties of the corresponding system. For example, in the case of a two-dimensional electronic system, a point defect produces oscillations in the LDOS with wavevector $2k_F$ for very low-bias volatge.[2] The period of these oscillations changes as a function of the bias voltage, from which one can infer the spectrum of the electrons. In the case of a superconductor, there can be additional features reflecting the symmetry of the superconducting gap.[3] Moreover, atomic manipulation permits the engineering of surfaces, making it possible to confine electrons into the so-called quantum corrals.[4] This has attracted great attention since it permits the study of lifetime effects, Kondo physics, single-atom gating, etc.[5] Very recently, open nanostructures have been shown to be amenable for quantum holographic encoding.[6] In the following we show that under suitable conditions, the LDOS exhibits oscillations due to the magnetic field that can be interpreted as due to the Aharonov-Bohm effect. Therefore the STM setup can be designed to serve as an Aharonov-Bohm interferometer at the nanometer scale.

For the sake of concreteness we consider the close-packed surface of a noble metal where the so-called Shockley surface states form a two-dimensional nearly free electron gas. Two atoms deposited on top of this surface can be modeled as two point scattering potentials for the surface electrons. This forms the simplest Aharonov-Bohm interferometer, where the role of the two different paths in conventional Aharonov-Bohm setups is played by the two scattering paths shown in Fig. 1. In the presence of a magnetic field, electrons scattering along these loops pick up different phases depending on whether the scattering is clockwise or anti-clockwise (the two paths being connected by time-reversal symmetry at zero field). This affects the interference contribution to the LDOS measured by the STM tip, which eventually exhibits oscillations as a function of the magnetic flux that passes through area enclosed by the above paths. The physics of these LDOS oscillations is similar to the effect of

the magnetic field on weak localization in disordered two-dimensional metals.[7]

The $dI(\mathbf{r}, V)/dV$ maps obtained experimentally are determined by the LDOS of the sample $N(\mathbf{r}, \omega = eV)$, the tip density of states, and the tunneling matrix elements.[5,8] In the Tersoff-Hamann approximation with a constant tip density of states dI/dV is proportional to N.[5,8] However, the oscillations of the LDOS that we discuss are picked up by the experimental dI/dV even if the above proportionality is lost due to voltage dependence of the tunneling matrix elements or due to variation in the tip density of states with energy. The LDOS of the sample can be obtained from the corresponding retarded Green's function as

$$N(\mathbf{r},\omega) = -\frac{2}{\pi}\mathrm{Im}\, G^R(\mathbf{r},\mathbf{r};\omega) \tag{1}$$

(the factor 2 is due to spin degeneracy). For a two-dimensional free-electron gas the Green's function is

$$G^R(\mathbf{r},\mathbf{r}';\omega) = -i\pi N H_0^{(1)}(k(\omega)|\mathbf{r} - \mathbf{r}'|). \tag{2}$$

Here $N = m/(2\pi\hbar^2)$ is the density of states of the electron gas per spin, $H_0^{(1)}$ is the zeroth-order Hankel function of the first
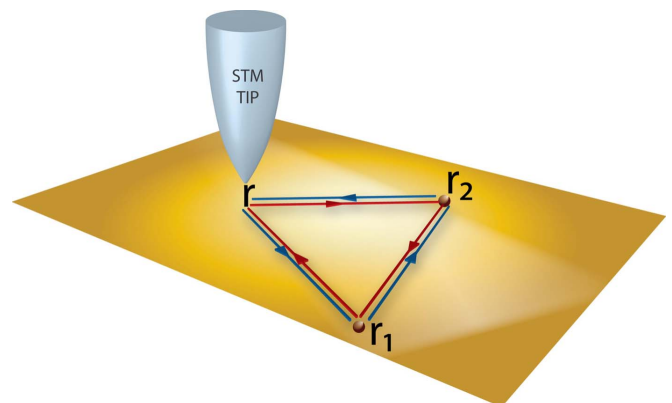

FIG. 1. (Color online) STM interferometer. $\mathbf{r}$ represents the position of the STM tip on the surface and $\mathbf{r}_1$ and $\mathbf{r}_2$ two impurities. The LDOS measured by the STM tip contains interference contributions due to electrons traveling along the two paths shown in the figure. The magnetic field affects this interference via the Aharonov-Bohm effect, producing oscillations in the LDOS that is measured by the tip.

kind and $k(\omega)$ is given by the dispersion relation $k(\omega) = k_F(1 + \omega/\mu)^{1/2}$, where $\mu = \hbar^2 k_F^2/(2m)$. For large distances $[r \gg k^{-1}(\omega)]$ we have

$$G^R(\mathbf{r}, \omega) \approx -iN\left(\frac{2\pi}{k(\omega)r}\right)^{1/2} e^{i[k(\omega)r - \pi/4]}. \quad (3)$$

The presence of impurities can be modeled by a term

$$H_{\text{imp}} = \int d\mathbf{r}\, U(\mathbf{r})\rho(\mathbf{r}) \quad (4)$$

in the Hamiltonian of the system, where U is the scattering potential associated with the impurities and ρ is the electronic density. Following a perturbative approach[5] the Green's function can be expressed as $G = G_0 + \delta G$, where G_0 is the Green's function in the absence of impurities and

$$\delta G(\mathbf{r}, \mathbf{r}') = \int d\mathbf{r}''\, G_0(\mathbf{r} - \mathbf{r}'') U(\mathbf{r}'') G_0(\mathbf{r}'' - \mathbf{r}')$$
$$+ \int\int d\mathbf{r}''d\mathbf{r}'''\, G_0(\mathbf{r} - \mathbf{r}'') U(\mathbf{r}'')$$
$$\times G_0(\mathbf{r}'' - \mathbf{r}''') U(\mathbf{r}''') G_0(\mathbf{r}''' - \mathbf{r}') + \dots \quad (5)$$

The dependence on the frequency is dropped since the scattering is assumed to be elastic. The latter quantity in Eq. (5) contains the interference contributions to the LDOS we are interested in (i.e., from terms second order and higher in the scattering potential).

Two identical point impurities are described by the scattering potential

$$U(\mathbf{r}) = U_0[\delta(\mathbf{r} - \mathbf{r}_1) + \delta(\mathbf{r} - \mathbf{r}_2)]. \quad (6)$$

In this case the quantity $\delta G(\mathbf{r}, \mathbf{r})$ naturally contains two types of terms. On one hand, there are (additive) terms in which the scattering with the impurities is produced separately. The Fourier transform of this contribution has quasiparticle peaks, which contains information about the dispersion of the electrons (see, e.g., Ref. 3). This contribution, however, plays no role in the physics that we intend to study. On the other hand, there are terms involving scattering with both the impurities. Among the latter terms, there are processes in which the semiclassical scattering paths enclose a finite area as in Fig. 1. It is important to note that such loops occur in pairs connected by time-reversal symmetry (i.e., clockwise and anticlockwise). For example, to the lowest order in the impurity potential, the contribution to the Green's function due to closed loops reads

$$\delta G_{\text{loop}}^{(2)}(\mathbf{r}, \mathbf{r}) = U_0^2 G_0(\mathbf{r} - \mathbf{r}_1) G_0(\mathbf{r}_1 - \mathbf{r}_2) G_0(\mathbf{r}_2 - \mathbf{r}) + (1 \leftrightarrow 2). \quad (7)$$

In the absence of a magnetic field the two terms in this expression are equivalent (due to time-reversal symmetry), and therefore give the same contribution to the LDOS (it can be said that the interference is constructive). In the presence of a magnetic field, however, time-reversal symmetry is broken. Then electrons traveling clockwise and anticlockwise along the above loop acquire different phases, so the subsequent interference is affected. This results in Aharonov-Bohm os-

cillations of the LDOS as we shall see explicitly below.

Next we demonstrate that the simple geometrical picture above remains unchanged when higher order terms in the impurity potential are taken into account. At higher order we have to deal with the following additional ingredients: (i) multiple scattering at the impurities and (ii) multiple scattering where semiclassically the particle goes back and forth between the two impurities. The first type of multiple scattering can be easily taken into account by replacing each of the scattering potentials by their respective T matrices. That is,[9]

$$U_0 \rightarrow \tilde{U}_0 = \frac{U_0}{1 - U_0 G_0(0)}. \quad (8)$$

As regards the second point, we note that $\delta G_{\text{loop}}(\mathbf{r}, \mathbf{r})$ is entirely due to processes where the path between the impurities is traversed an odd number of times (otherwise the scattering path does not enclose a finite area). In the second order contribution Eq. (7), for example, the path between the impurities is traversed once. At $\mathcal{O}(U_0^4)$ there are contributions where the path is traversed three times, and so on. Taking all this into account, we obtain

$$\delta G_{\text{loop}}(\mathbf{r}, \mathbf{r}) = W^2 G_0(\mathbf{r} - \mathbf{r}_1) G_0(\mathbf{r}_1 - \mathbf{r}_2) G_0(\mathbf{r}_2 - \mathbf{r}) + (1 \leftrightarrow 2), \quad (9)$$

where

$$W^2 = \frac{\tilde{U}_0^2}{1 - \tilde{U}_0^2 G_0(\mathbf{r}_1 - \mathbf{r}_2) G_0(\mathbf{r}_2 - \mathbf{r}_1)}. \quad (10)$$

It is worth noticing that in all the processes that finally give rise to Eq. (9) we are actually dealing with the same area, since to go back and forth along the same line, for example, does not change the area of the resulting loop. This is the simple reason why the nontrivial phase relation between the clockwise and the anticlockwise paths in the presence of a magnetic field is not washed out by multiple impurity scattering.

Let us now consider explicitly the influence of the magnetic field. In the low-field regime (see below) we can use the semiclassical approximation for the electron Green's function:[7]

$$G_0(\mathbf{r} - \mathbf{r}') = \exp\left(i\frac{\pi}{\Phi_0}\int_{\mathbf{r}}^{\mathbf{r}'} \mathbf{A}(\mathbf{l}) \cdot d\mathbf{l}\right) G_{00}(\mathbf{r} - \mathbf{r}'). \quad (11)$$

Here $G_{00}(\mathbf{r} - \mathbf{r}')$ represents the Green's function in the absence of magnetic field, $\mathbf{A}$ is the vector potential ($\mathbf{B} = \nabla \times \mathbf{A}$), $\Phi_0 = h/(2e)$ is the flux quantum, and the integral is along the straight line connecting $\mathbf{r}$ and $\mathbf{r}'$. The magnetic field then enters the interference contributions to the LDOS via complex factors $e^{\pm i\pi\Phi/\Phi_0}$, where Φ is the magnetic flux through the area enclosed by the corresponding scattering path (the different signs of the phase corresponds to anticlockwise and clockwise line integrals respectively). As a result, the LDOS can be written as
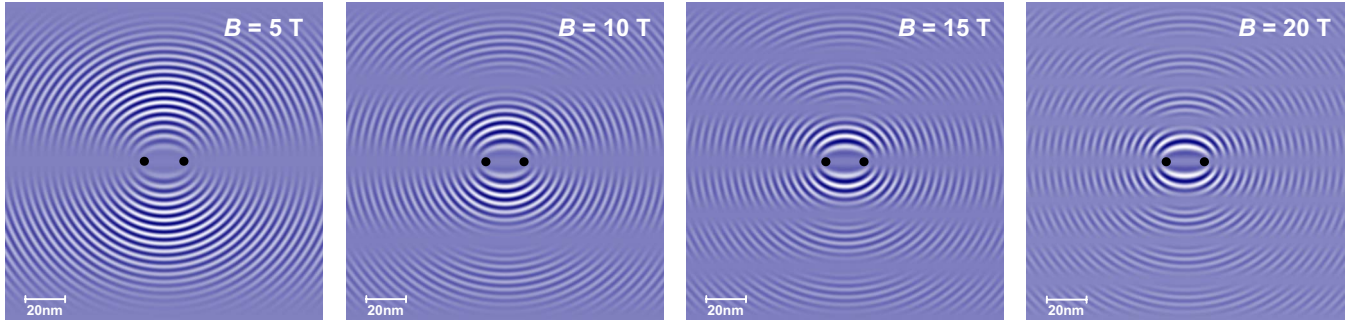
FIG. 2. (Color online) Expected STM patterns for two impurities 20 nm apart on the Ag(111) surface after subtraction of the $B=0$ signal. The horizontal stripes are produced by the Aharonov-Bohm effect in the LDOS, whereas the remaining elliptic features are due to the interference contributions described by N_{loop} [with $\lambda_F=7.6$ nm and real W matrices as defined in Eq. (10)].

$$N(\mathbf{r},\omega) = N_{B=0}(\mathbf{r},\omega) + N_{\mathrm{loop}}(\mathbf{r},\omega)[\cos(\pi\Phi/\Phi_0)-1],$$
$$(12)$$

where $N_{B=0}$ is the zero-field total LDOS and

$$N_{\mathrm{loop}}(\mathbf{r},\omega) = -\frac{2}{\pi}\mathrm{Im}\ \delta G_{\mathrm{loop}}(\mathbf{r},\mathbf{r};\omega) \qquad (13)$$

represents the (constructive) interference contribution due to all closed paths in the absence of a magnetic field [computed from Eq. (9) with G_{00}]. This interference process picks up a nontrivial phase in the presence of a magnetic field, giving rise to oscillations in the LDOS as in Eq. (12), which is a manifestation of the Aharonov-Bohm phenomenon.[10] This can be revealed by varying either the magnetic field or the relative position between the STM tip and the impurities since Φ changes in both cases. We note that, irrespective of the position of the STM tip, the magnitude of the correction to the LDOS reduces with B for low magnetic fields. As in the case of negative magnetoresistance in weak localization, this is due to the fact that magnetic field induces destructive interference between the contribution of the two semiclassical paths.

Next we discuss the limitations of our calculations and the feasibility of our proposal to use the STM as an Aharonov-Bohm interferometer at a nanometer scale. The expression (12) for the LDOS has been derived within a semiclassical approach, so it holds as long as Eq. (11) can be used for describing the influence of the magnetic field on the electron system. This is possible if the magnetic field is such that the Fermi wavelength is much smaller than the Landau orbits:

$$\lambda_F \ll a_B = \left(\frac{\Phi_0}{\pi B}\right)^{1/2}. \qquad (14)$$

The magnetic field needed to observe a complete Aharonov-Bohm oscillation can be estimated as

$$B_{2\pi} \sim 4\Phi_0/d^2, \qquad (15)$$

where d is the characteristic distance in the setup, i.e., the distance between the impurities and/or between the impurities and the position of the tip. For $d\sim 40-20$ nm this field is $B_{2\pi}\sim 5-20$ T, which corresponds to Landau orbits $a_B \sim 11-6$ nm. For Cu(111) and Ag(111) $\lambda_F=2.95$ nm and 7.6 nm, respectively, and therefore the condition in Eq. (14) for

the semiclassical approximation is valid. Furthermore, in spite of the fact that the interference signal is long-range in the sense that N_{loop} decays as $1/d$ in a power-law fashion [see Eq. (3)], in reality there are dephasing processes that introduce an extra attenuation (thermal dephasing for example), and which, for simplicity, have not been taken into account in the current computation. Experimentally, in fact, the impurity-induced variations in the LDOS are typically observed up to distances of the order of a few times the Fermi wavelength, say $10\lambda_F$.[11] Therefore the characteristic distance in our setup must be $d\lesssim 10\lambda_F$. For $d\sim 40-20$ nm we then need $\lambda_F\gtrsim 4-2$ nm, which still can be smaller than a_B at 5–20 T. Thus we find that the semiclassical interpretation is good to describe the first few periods of the LDOS oscillations. The first corrections to our results will be due to the curvature of the classical trajectories, which can still be described within the semiclassical picture.[12] To describe sufficiently high periods, however, one has to go beyond Eq. (11) and consider the influence of the magnetic field within a Landau-level approach. These periods imply magnetic fields considerably high (>20 T), so we do not develop this latter approach here.

The Aharonov-Bohm physics reveals also in the spatial variations of the LDOS for a fixed magnetic field. In our setup Φ varies only in the direction perpendicular to the line connecting the two impurities. In consequence, the STM scans along this direction will show a periodic envelope due to the cosine factor in Eq. (12). With two impurities separated 20 nm, fields of 5–20 T give rise to periods of 80 and 20 nm, respectively, for such an envelope (see Fig. 2).

It is also worth mentioning that the Zeeman splitting, neglected so far, has a trivial influence on the Aharonov-Bohm oscillations if the spin is conserved in the scattering process. N_{loop} in Eq. (12) actually results from contributions associated with the two spin polarizations. It can be written as $N_{\mathrm{loop}}=\frac{1}{2}(N_{\mathrm{loop}}^{\uparrow}+N_{\mathrm{loop}}^{\downarrow})$ if the spin is conserved. The eventual difference between $N_{\mathrm{loop}}^{\uparrow}$ and $N_{\mathrm{loop}}^{\downarrow}$ due to the Zeeman splitting can be probed by means of spin-polarized STM. However this difference does not alter the oscillatory behavior of the LDOS described above. The situation is more subtle if the spin can flip during the scattering process as a result of, e.g., spin-orbit coupling. This can affect multiple scattering in a nontrivial way,[13] and can give rise to the analog of the antilocalization phenomenon if spin components are measured separately.

In summary, we have shown that magnetic field affects electron interference contributions to the local density of states via the Aharonov-Bohm effect. This can be exploited in building STM devices that serve as Aharonov-Bohm interferometers at the nanometer scale. We have illustrated this possibility for the close-packed surface of a noble metal with two atoms adsorbed on top. The role of these atoms consists in creating strong enough scattering potentials, which can also be produced, for example, using additional STM tips.

The implementation of this new functionality into the STM technique might broaden its applications notably, offering new perspectives for STM studies of the fundamental properties of surfaces and underlying systems.

*cano@esrf.fr

†indranil.paul@grenoble.cnrs.fr

[1] C. J. Chen, *Introduction to Scanning Tunneling Microscopy* (Oxford, New York, 1993).

[2] M. F. Crommie, C. P. Lutz, and D. M. Eigler, Nature (London) **363**, 524 (1993); Y. Hasegawa and Ph. Avouris, Phys. Rev. Lett. **71**, 1071 (1993).

[3] J. M. Byers, M. E. Flatté, and D. J. Scalapino, Phys. Rev. Lett. **71**, 3363 (1993).

[4] M. F. Crommie, C. P. Lutz, and D. M. Eigler, Science **262**, 218 (1993).

[5] G. A. Fiete and E. J. Heller, Rev. Mod. Phys. **75**, 933 (2003).

[6] C. R. Moon *et al.*, Nat. Nanotechnol. **4**, 167 (2009).

[7] B. L. Altshuler, D. Khmelnitzkii, A. I. Larkin, and P. A. Lee, Phys. Rev. B **22**, 5142 (1980); G. Bergmann, Phys. Rep. **107**, 1 (1984).

[8] J. Tersoff and D. R. Hamann, Phys. Rev. Lett. **50**, 1998 (1983); Phys. Rev. B **31**, 805 (1985); J. M. Blanco, F. Flores, and R. Perez, Prog. Surf. Sci. **81**, 403 (2006); O. Fischer *et al.*, Rev. Mod. Phys. **79**, 353 (2007).

[9] Expression (2) gives a spurious divergence for the real part of $G(\mathbf{r}, \omega)$ for $\mathbf{r}=0$. This divergence is regularized by using Kramers-Kroning relations to define the real part of $G(0, \omega)$ in expression (8) as Re $G(0, \omega) = -\frac{2}{\pi}\mathbb{P}\int\frac{\text{Im } G(0,\omega')}{\omega-\omega'}d\omega'$ and by cutting off the integral with the corresponding electron bandwidth [see, e.g., S. Doniach and E. H. Sondheimer, *Green's Functions for Solid Physicists* (W.A. Benjamin Inc., London, 1974), p. 79].

[10] Note that the experimental dI/dV maps will show the Aharonov-Bohm oscillations even if dI/dV is not proportional to the local density of states of the sample.

[11] In the case of Cu(111) and Ag(111) the phase relaxation length can be as large as 66 and 60 nm, respectively, at low temperatures [see, e.g., O. Jeandupeux, L. Burgi, A. Hirstein, H. Brune, and K. Kern, Phys. Rev. B **59**, 15926 (1999)].

[12] T. A. Sedrakyan, E. G. Mishchenko, and M. E. Raikh, Phys. Rev. Lett. **99**, 036401 (2007).

[13] J. D. Walls and E. J. Heller, Nano Lett. **7**, 3377 (2007).